Identification of Dipeptidyl Nitriles as Potent and Selective Inhibitors of Cathepsin B through Structure-Based Drug Design

Paul D. Greenspan,* Kirk L. Clark, Ruben A. Tommasi, Scott D. Cowen, Leslie W. McQuire, David L. Farley, John H. van Duzer, Ronald L. Goldberg, Huanghai Zhou, Zhengming Du, John J. Fitt, David E. Coppa, Zheng Fang, William Macchia, Lijuan Zhu, Michael P. Capparelli, Robert Goldstein, Andrew M. Wigg, John R. Doughty, Regine S. Bohacek, and Ania K. Knap

Arthritis and Bone Metabolism Research, Novartis Pharmaceuticals Corporation, 556 Morris Avenue, Summit, New Jersey 07901

Received May 9, 2001

Cathepsin B is a member of the papain superfamily of cysteine proteases and has been implicated in the pathology of numerous diseases, including arthritis and cancer. As part of an effort to identify potent, reversible inhibitors of this protease, we examined a series of dipeptidyl nitriles, starting with the previously reported Cbz−Phe−NH−CH_2CN (**19**, IC_{50} = 62 μM). High-resolution X-ray crystallographic data and molecular modeling were used to optimize the P_1, P_2, and P_3 substituents of this template. Cathepsin B is unique in its class in that it contains a carboxylate recognition site in the S_2' pocket of the active site. Inhibitor potency and selectivity were enhanced by tethering a carboxylate functionality from the carbon α to the nitrile to interact with this region of the enzyme. This resulted in the identification of compound **10**, a 7 nM inhibitor of cathepsin B, with excellent selectivity over other cysteine cathepsins.

Introduction

Cathepsin B (cat B) is a lysosomal cysteine protease, which belongs to the papain superfamily.[1] It is an ubiquitously expressed protein (in contrast to its more highly regulated relatives, such as cat S or cat K)[2] and has long been thought to function primarily in normal intracellular protein turnover.[3] However, more recent studies have implicated cat B in the pathology of a number of important human diseases, including cancer[4] and neurodegenerative disorders.[5] Cat B has been shown to be upregulated in patients with rheumatoid arthritis,[6] and components of the extracellular matrix are known to be substrates for this enzyme.[7] Unselective cysteine cathepsin inhibitors have previously been reported to be effective in animal models of rheumatoid arthritis.[8]

The majority of cysteine protease inhibitors are peptidic or peptidomimetic compounds in which the hydrolyzable amide is replaced by an electrophilic functionality. In this way, the catalytic thiol of the enzyme reacts with the inhibitor to form a covalent complex.[9] Until recently, most potent cysteine protease inhibitors were irreversible inhibitors, in which the electrophilic "warhead" alkylates the enzyme, through nucleophilic displacement or conjugate addition. Examples of this approach include fluoromethyl ketones, acyloxymethyl ketones, vinyl sulfones, or epoxysuccinates.[10] Alternatively, potent, reversible inhibition can be achieved through highly electrophilic warheads such as aldehydes or α-ketoamides, which form reversible, covalent bonds to the active site thiol.[10] Recently, researchers at SmithKline Beecham have reported hydrazides[11] and *bis*-α-amidoketones[12] as potent inhibitors of cat K, resulting from elegant structure-based optimization. These compounds bind in a manner similar to that of aldehydes and ketoamides.

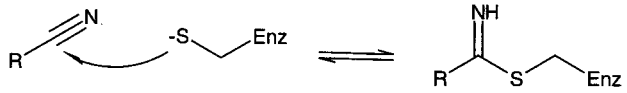

Figure 1. Mechanism of nitrile inhibition of cysteine proteases.

This paper will describe our initial efforts toward identification of potent peptidyl nitrile inhibitors of cat B. Representatives of this class of compounds have long been known to inhibit cysteine proteases.[10] Nuclear magnetic resonance (NMR) studies indicate that this inhibition occurs through the formation of a thioimidate intermediate (Figure 1) and that this process is fully reversible.[13] Mutation studies have suggested that this intermediate is stabilized by a neighboring Gln residue,[14] which, along with the backbone NH of the catalytic cysteine residue, forms the putative "oxyanion hole" of the enzyme.[15] However, there are no reports to date of highly potent nitrile inhibitors of cysteine proteases (IC_{50} or $K_i \ll 1$ μM) and very few of inhibition of a cysteine cathepsin by this class of inhibitor.[16−18] It was apparent, therefore, that substantial optimization of the template would be necessary to provide adequate potency.

Chemistry

All of the compounds discussed are based on a dipeptidyl nitrile scaffold. Compounds with no substituent α to the nitrile, such as **3**, were prepared using the procedure shown in Scheme 1. A Boc-protected amino acid **2** was coupled to aminoacetonitrile under standard conditions. After amine deprotection, acylation with the

* To whom correspondence should be addressed. Tel: (908)277-4775. Fax: (908)277-4885. E-mail: paul.greenspan@pharma.novartis.com.

10.1021/jm010206q CCC: $20.00
Published on Web 11/14/2001

Scheme 1. Representative Synthesis of Dipeptidyl Nitriles with No α-Substituent[a]

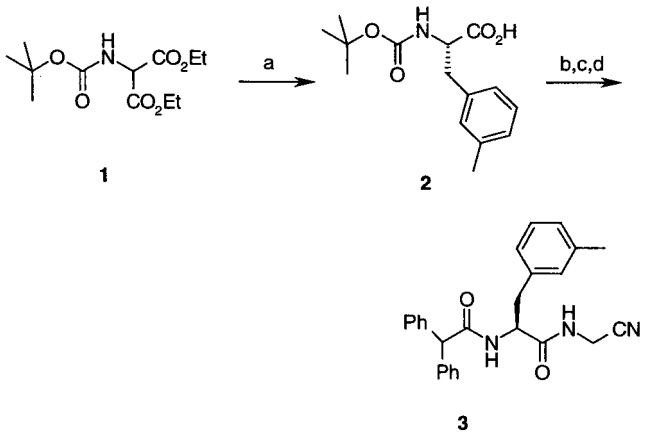

[a] (a) 3-Methylbenzyl bromide, NaH, DMF, room temperature, then AcOH, reflux, then alcalase 2.4 L; (b) aminoacetonitrile·HCl, EDCI, HOBt, NMM, CH_2Cl_2; (c) HCOOH, then aqueous $NaHCO_3$; (d) Ph_2COCl, NMM, CH_2Cl_2.

Scheme 2. Synthesis of N-Substituted Nitrile[a]

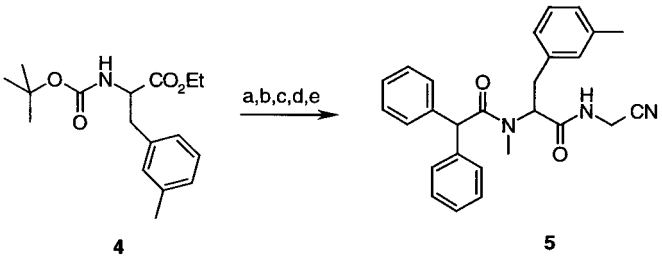

[a] (a) NaH, MeI, DMF; (b) HCl, EtOAc; (c) diphenylacetyl chloride, NMM, CH_2Cl_2; (d) LiOH, THF, water; (e) aminoacetonitrile·HCl, EDCI, HOBt, NMM, CH_2Cl_2.

appropriate capping group yielded the desired product **3**. Racemic Boc-protected amino acids that were not commercially available were prepared using standard aminomalonate alkylation chemistry, as shown in Scheme 1.[19] Where optically active amino acids were required, the racemic Boc amino esters were resolved via enzymatic hydrolysis[20] to produce the (S)-enantiomer as the free acid, in >98% ee. In these cases, the alkylation, malonate decarboxylation, and subsequent enzymatic hydrolysis were all performed in one pot, resulting in very efficient generation of the requisite amino acids.

The N-alkylated nitrile **5** was prepared via the racemic ethyl ester **4** (Scheme 2). After N-methylation and cleavage of the *tert*-butylcarbamate, the amino ester was acylated, hydrolyzed, and coupled with aminoacetonitrile to yield **5**.

In other cases, it was necessary to first prepare a substituted aminonitrile fragment before assembling the final product. Benzyloxymethyl-substituted amino nitriles, exemplified by compound **9**, were prepared through alkylation of the dianion of Boc L-serine with an appropriately substituted benzylic halide, such as **7** (Scheme 3). The resulting amino acid was converted to primary amide **8**, which was subsequently dehydrated and deprotected to yield **9**. This aminonitrile was then subjected to a sequence similar to that described previously. Pd(0)-catalyzed deprotection of the allyl ester was accomplished in the final step to yield **10**.

To synthesize arylpropyl-tethered nitriles such as **14**, the diprotected propargyl glycine **11** was first prepared as previously reported[21] (Scheme 4). The terminal acetylene was then coupled with methyl 3-bromobenzoate and subjected to alcalase hydrolysis to yield the (S)-enantiomer of acid **12**, in >97% ee. The free acid was then converted to its corresponding primary amide and deprotected, yielding **13**. This intermediate was carried on as before to yield, after ester deprotection,[22] compound **14**.

Aryl ether-substituted amino nitrile **17** was prepared from methyl 3-hydroxybenzoate **15** via O'Donnell type alkylation[23] of iodoether **16**. Racemic **17** was employed in this case, yielding **18** as a 1:1 mixture of isomers at the P_1 position (Scheme 5).

Results and Discussion

As a starting point, we prepared compound **19** (Table 1), which was previously reported to be a sub-micromolar inhibitor of bovine cat B.[16] In our hands, against the recombinant human enzyme, the compound was found to be much less potent, with an IC_{50} of 62 μM. To generate a molecular model of inhibitor binding, we employed the coordinates of the structure of recombinant rat cat B bound to the irreversible inhibitor Z-Arg-Ser(OBn)-CMK.[24] We were confident that the use of the rat enzyme would not compromise our modeling work, since the active site contained only two point mutations: Ser175Thr (at the base of the S_2 pocket, remote to any simple aromatic P_2 substituent) and Glu122Gly (in a highly disordered portion of the occluding loop). It was felt that the peptidyl nitrile inhibitor would bind in an orientation similar to this chloromethyl ketone, since they were both covalently linked peptidic inhibitors. Because it had previously been established that peptidyl nitriles bind through formation of a thioimidate ester intermediate,[13] we incorporated this linkage into our enzyme−inhibitor model. Using a subset of the enzyme (including residues ~12 Å from the center of the binding site), the model was subjected to Monte Carlo docking using the McDock algorithm of the QXP molecular modeling suite.[25] During minimizations, the side chains of Gln 23, Cys 29, Tyr 75, Glu 122, Glu 245, and His 199 were allowed to be flexible, and the covalent bond from Cys 29 to the inhibitor was maintained. The predicted lowest energy conformation, depicted in Figure 2, was consistent with the mode of binding observed in the crystal structure of rat cat B bound to Z-Arg-Ser-(OBn)-CMK.[24] The S_2 and S_3 subsites are occupied by the Phe and Cbz groups, respectively, and hydrogen-bonding interactions are formed from the P_1 and P_2 amide NHs and from the P_2 carbonyl to the enzyme. If one assumes that this is the correct binding mode, then close inspection clearly reveals several structural aspects that can be exploited to improve potency in this template. The most obvious of these are the suboptimal occupancy of the S_2 and S_3 pockets of the enzyme and complete absence of binding into the S′ side of the active site.

To optimize this inhibitor, we decided to retain the peptidic template so as to preserve the key backbone H-bond interactions with the enzyme. We then chose to take a modular approach toward optimization, in which substituents would be modified iteratively, based

Scheme 3. Preparation of Aminonitriles Containing a Benzyloxymethyl Substituent[a]

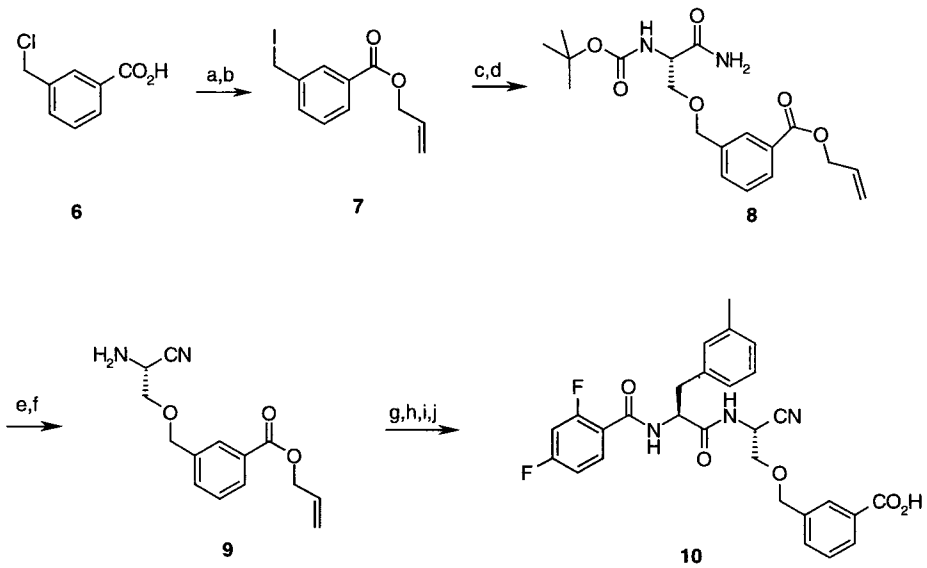

[a] (a) K_2CO_3, acetone, reflux; (b) NaI, acetone; (c) Boc-serine, 2 NaH, DMF, 0 °C; (d) $ClCO_2{}^iBu$, NMM, CH_2Cl_2, −15 °C, then NH_3, room temperature; (e) $(COCl)_2$, DMF, pyridine; (f) HCOOH, then aqueous $NaHCO_3$; (g) **2**, EDCI, HOBt, NMM, CH_2Cl_2; (h) HCOOH, then aqueous $NaHCO_3$; (i) 2,4-difluorobenzoyl chloride, NMM, CH_2Cl_2; (j) morpholine, $Pd(PPh_3)_4$, THF.

Scheme 4. Preparation of Arylpropyl-Substituted Aminonitriles[a]

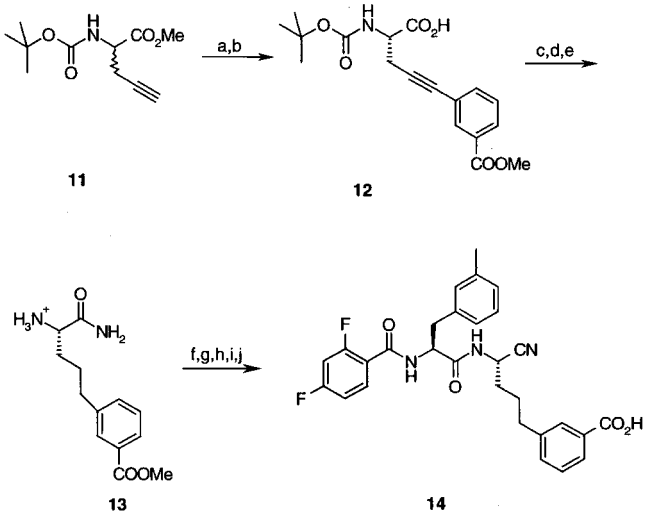

[a] (a) Methyl 3-bromobenzoate, CuI, $(Ph_3P)_2PdCl_2$, TEA; (b) alcalase 2.4 L, MeCN, 0.2 M $NaHCO_3$; (c) $ClCO_2{}^iBu$, NMM, CH_2Cl_2, −15 °C, then NH_3, room temperature; (d) H_2, 10% Pd/C, EtOH, 1 atm; (e) HCl, EtOAc; (f) **1**, EDCI, HOBt, NMM, CH_2Cl_2; (g) (c) $(COCl)_2$, DMF, pyridine; (h) HCOOH, then aqueous $NaHCO_3$; (i) 2,4-difluorobenzoyl chloride, NMM, CH_2Cl_2; (j) potassium trimethylsilanoate, CH_2Cl_2.

Scheme 5. Preparation of Aryloxyethyl Subsituted Aminonitriles[a]

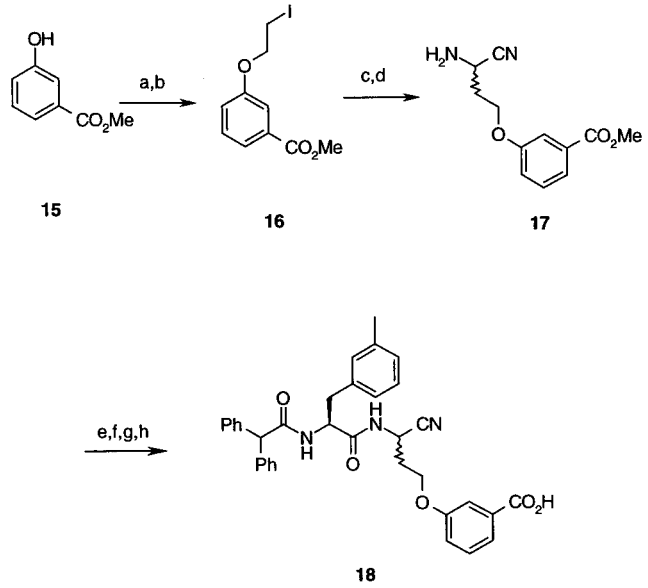

[a] (a) 1,2-Dibromoethane, K_2CO_3, acetone, reflux; (b) NaI, acetone, reflux; (c) *N*-(diphenylmethylene)aminoacetonitrile, $NaN(TMS)_2$, THF, −78 °C to room temperature; (d) 1 N HCl, Et_2O; (e) **1**, EDCI, HOBt, NMM, CH_2Cl_2; (f) HCOOH, then aqueous $NaHCO_3$; (g) diphenylacetyl chloride, NMM, CH_2Cl_2; (h) potassium trimethylsilanoate, THF.

on structural information. Starting with the P_3 acyl substituent (Table 1), it was observed that the CBz phenyl group of compound **19** was tethered too far from the P_2−P_3 amide to interact optimally with Tyr 75, which is the most prominent feature in the S_3 pocket. Removal of the oxygen from the CBz group to reduce the phenyl tether length resulted in a modest increase in potency (**20**). However, a ~100-fold improvement was observed upon replacing the phenylacetyl group with a diphenylacetyl to further occupy this hydrophobic pocket, thus producing a 0.5 μM cat B inhibitor (**21**).

Before undertaking a substantial characterization of the P_3 substituent structure−activity relationship (SAR), attention was turned to the P_2 position. Examination of the aromatic ring within the S_2 binding site suggested that there was room for an additional hydrophobic moiety attached to the phenyl group. Because a substituent at the meta position appeared to be most favored in the model, several 3-substituted phenylalanine-containing compounds were prepared, initially in racemic form. 3-Iodo substitution led to a 4-fold enhancement in potency (**22**). Consistent with our modeling results, the 4-iodo compound was found to be inactive (**23**). A survey of other small hydrophobic groups indicated that the methyl substituent was

Table 1. Dipeptidic Nitriles Containing No P_1 Substituent

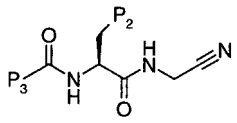

cmpd	P_3	P_2	IC_{50} (nM)
19	$PhCH_2O$	Ph	62 000[b]
20	$PhCH_2$	Ph	34 000[b]
21	Ph_2CH	Ph	496 ± 108
22	Ph_2CH	3-iodophenyl[a]	121 ± 38
23	Ph_2CH	4-iodophenyl	>1000[b]
24	Ph_2CH	3-methylphenyl[a]	87 ± 26
25	PH_2CH	3-chlorophenyl[a]	130 ± 34
26	Ph_2CH	3-ethylphenyl[a]	136 ± 26
3	Ph_2CH	3-methylphenyl	45 ± 7.6
27	Ph	3-methylphenyl[a]	1900[b]
28	*n*-Bu	3-methylphenyl	3000[b]
29	4-chlorophenyl	3-methylphenyl	308 ± 35
30	2,4-difluorophenyl	3-methylphenyl	591[b]
31	3,4-dichlorophenyl	3-methylphenyl	31.3 ± 1.3
32	2-fluoro-4-chlorophenyl	3-methylphenyl	72[b]
34	Ph_2CH	3,5-dimethylphenyl[a]	11.9 ± 2.3
35	Ph_2CH	3-(NH_2CH_2)-5-Me-Ph[a]	358 ± 8.5
36	Ph_2CH	3-amidinoPh[a]	>1000[b]
37	Ph_2CH	3-(5-methylpyridyl)[a]	652 ± 28

[a] The compound is racemic. [b] $n = 1$.

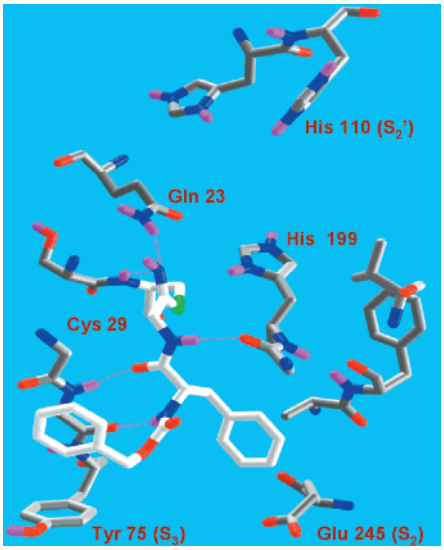

Figure 2. Compound **19** modeled into rat cat B active site.

marginally better than the others (**24**−**26**). Preparation of the (*S*)-isomer of this compound identified **3** as a 45 nM inhibitor of cat B.

At this point, the P_3 SAR was further explored. An unsubstituted benzamide (**27**, a racemate) showed only weak activity in comparison to **3**, as did an alkyl substituent (**28**), again presumably due to inadequate interaction with Tyr 75. However, incorporation of a para-chloro substituent (**29**) led to a substantial increase in potency over **27**. Additional incorporation of a 3-chloro or 2-fluoro (**31** and **32**, respectively) led to compounds with potencies similar to or better than **3**, further highlighting the importance of an appropriate hydrophobic aromatic substituent in this position.

Cocrystallization experiments were then carried out with recombinant human cat B and compound **3**. Diffraction data were collected at cryogenic temperatures, and the crystal structure was fully refined to an *R* factor

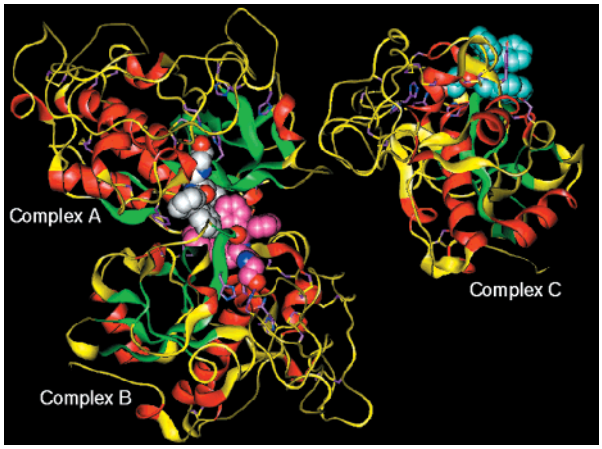

Figure 3. Overview of cat B−**3** complex X-ray structure.

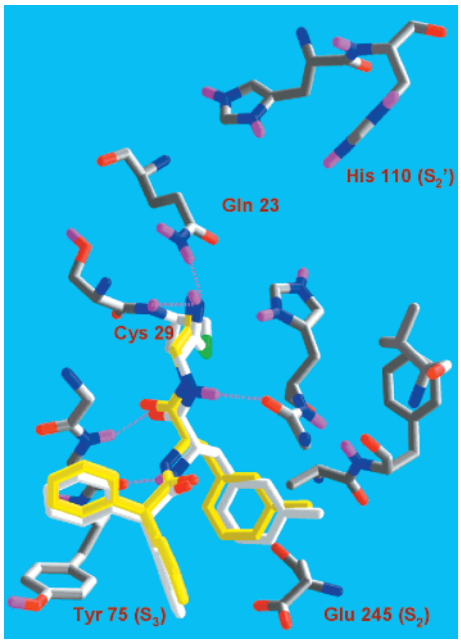

Figure 4. X-ray structure of compound **3** in cat B active site, overlaid with modeling prediction generated from rat cat B X-ray structure.

of 15.9% at a resolution of 1.9 Å. The asymmetric unit in this crystal form contains three independent enzyme−inhibitor complexes, which are nearly identical with respect to the active site and inhibitor. Two of these complexes contacted each other near their active sites in a pseudo-C_2 symmetric fashion. This proximity raised some concern that crystal packing could be influencing the bound inhibitor conformation (Figure 3). Fortunately, however, the third enzyme in the asymmetric unit was fully solvent exposed and served to confirm the validity of the observed binding orientations. Figure 4 displays the experimental enzyme−inhibitor complex overlaid with the lowest energy structure predicted using molecular modeling. It is evident that there was excellent agreement between the results of molecular modeling and the results of X-ray crystallography, thus giving us confidence that we could use our model in a predictive manner. The crystal structure provided us with the opportunity to critically examine the ligand's covalent bond to the active site cysteine as well as its nonbonded interactions with the enzyme.

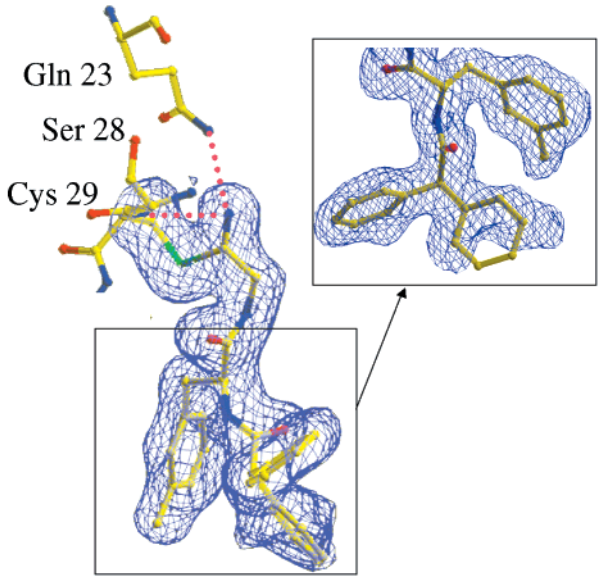

Figure 5. Electron density map of cat B−**3** structure illustrating the mode of interaction of the nitrile functionality with the catalytic site of the enzyme. Fo−Fc electron density map with inhibitor and Cys 29's CB and SG atoms omitted from Fc. Inset panel has been rotated to better show the P2 and P3 ring systems.

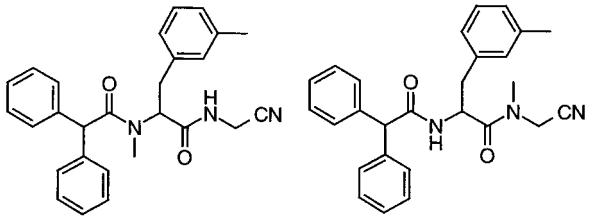

Figure 6. N-substituted dipeptidyl nitriles (both inactive against cat B at 10 μM).

The high-resolution crystal structure demonstrated conclusively that the nitrile inhibitor binds through formation of a thioimidate ester with Cys 29 of the cat B active site. The thioimidate nitrogen was clearly planar and sp^2 hybridized. In addition, this structure confirms the role of the backbone NH of Cys 29 and the side-chain amide of Gln 23 in stabilization of the intermediate (Figure 5) with hydrogen bond distances of 3.1 and 3.0 Å, respectively.

The backbone hydrogen-bonding pattern predicted through modeling was observed in the crystal structure. This result was further verified by the observation that compounds methylated at either NH had no measurable cat B activity (**5** and **33**, Figure 6).

As anticipated, one phenyl group of the P_3 diphenylacetyl moiety appears to form a favorable edge-to-face interaction with Tyr-75, and its position is well-defined by the electron density in the crystal structure. The weak electron density for the second P_3 aromatic ring indicates that its orientation is not well-defined (Figure 5); however, the SAR data indicate that this group is essential for high potency. The high potency seen with other hydrophobic substituents at P_3 (compounds **31** and **32**) indicates that this result may simply be due to increased desolvation energy.

One of the most intriguing observations was that the positioning of the 3-methyl group on the P_2 phenylalanine within the cat B active site was ambiguous, since two of the complexes in the unit cell showed methyl group density on opposite sides of the phenyl ring, and the third was not definitive. This led us to prepare the dimethylated compound **34** (racemate), which was found to be 4-fold more potent than **3**.

The S_2 pocket of cat B also contains a glutamate residue (Glu 245), which has previously been demonstrated to provide the enzyme with the ability to recognize substrates with positively charged P_2 residues.[26] The crystal structure shows clearly that this carboxylate residue is able to rotate out of the way of an aromatic substituent in order to avoid an unfavorable interaction. We were hopeful that we could capitalize on this structural feature by incorporating positive charge into the P_2 substituent. Unfortunately, we were unsuccessful in this endeavor, as inhibitors with an aminomethyl substituent (**35**), an amidino group (**36**), or a 3-pyridylalanyl P_2 moiety (**37**) were all less potent than the 3-methylphenylalanyl. There is currently no satisfactory explanation for the failure of this approach, although it does serve to highlight the sometimes empirical nature of structure-based drug design.

The inhibitors thus far discussed bind solely into the S_2 and S_3 pockets of the enzyme active site, assuming that the observed binding mode for inhibitor **3** is unchanged throughout the series. If this is correct, then the large S_2' portion of the enzyme is completely vacant. This site is very important when designing inhibitors of cat B, since this enzyme has an S′ pocket that is unique among papain superfamily proteases. Other cathepsins, such as cat L, S, and K, have relatively open S′ regions, whereas in cat B this region is blocked by a 19-residue insertion.[27] His 110 and His 111 in this insertion have previously been shown to bind carboxylate groups,[28] thus providing cat B with its unusual C-terminal dipeptidyl exopeptidase activity.[29] We sought to exploit this binding pocket to further improve the potency of the inhibitors.

A limitation of a nitrile-based inhibitor template is the fact that the nitrile is a terminating functionality, which, unlike a ketone or hydrazide, for example, only allows for elaboration in one direction. However, examination of the enzyme−inhibitor crystal structure led us to hypothesize that the histidine region of S′ could be accessed via P_1 substitution. Previous reports have indicated that O-benzyl serine is tolerated in the P_1 position of cat B inhibitors.[30] In our series, incorporation of this substituent led to a 5-fold enhancement in binding (**38**, Table 2), as compared to compound **3**. Modeling of compound **38** into the cat B active site shows that the phenyl group is likely to be positioned into a shallow hydrophobic pocket. This prediction is consistent with the X-ray structure of the chloromethyl ketone discussed previously.[24] In this orientation, it appeared that placement of a carboxylate in the meta-position of the pendant aromatic ring would allow for a salt-bridging interaction with one of the histidines of the occluding loop (Figure 7). Indeed, this carboxylated compound (**39**) was found to be highly potent, with an IC_{50} of 1.8 nM. The importance of the placement of the carboxylate was confirmed when the para-carboxylate

Table 2. Dipeptidic Nitriles with P_1 Substitution

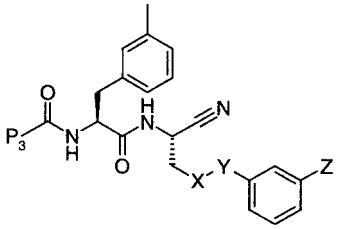

cmpd	P_3	X	Y	Z	IC_{50} (nM)
38	Ph_2CH	O	CH_2	H	10.2 ± 0.6
39	Ph_2CH	O	CH_2	3-COOH	1.8 ± 0.75
40	Ph_2CH	O	CH_2	4-COOH	30.7 ± 3
41	Ph_2CH	O	CH_2	3-CH_2OH	29[b]
42	Ph_2CH	O	CH_2	3-COOMe	47[b]
43	Ph_2CH	CH_2	CH_2	3-COOH	18[b]
18	Ph_2CH	CH_2	O	3-COOH	138[b,c]
44	Ph_2CH	C≡C		3-COOH	5.6 ± 2.7
45	Ph_2CH	O	CH_2	5-COOH[a]	5.0 ± 1.5
46	2-fluoro-4-chlorophenyl	O	CH_2	H	16.9 ± 0.4
47	2-fluoro-4-chlorophenyl	O	CH_2	3-COOH	2.0 ± 0.1
48	Ph	O	CH_2	3-COOH	9.4 ± 1.6
49	*n*-Bu	O	CH_2	3-COOH	35.7 ± 7.2
10	2,4-difluorophenyl	O	CH_2	3-COOH	6.8 ± 0.6
14	2,4-difluorophenyl	CH_2	CH_2	3-COOH	110 ± 17
50	2,4-difluorophenyl	O	CH_2	H	42, 43[d]

[a] Substituent is 5-carboxy-2-furyl. [b] $n = 1$. [c] At P_1, there is a 1:1 mixture of diastereomers. [d] $n = 2$.

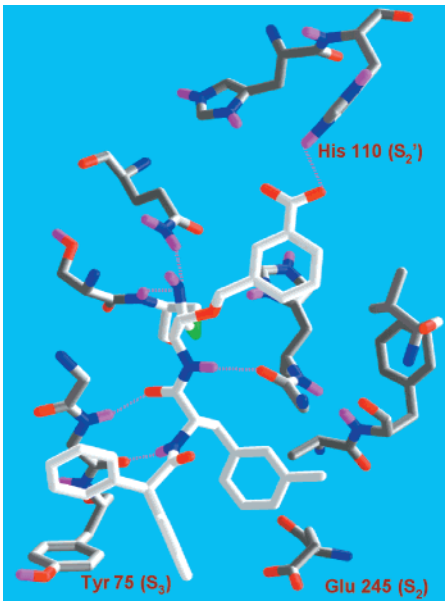

Figure 7. X-ray structure of compound **35** modeled into cat B active site.

isomer (**40**) was found to be roughly 15-fold less potent than **39.** The fact that **40** is 3-fold less potent than **38** may be explained by a decrease in desolvation energy for compound **40**, since the carboxylate functionality should increase its water solubility. The requirement for an acidic functionality in the meta-position was confirmed by the reduced potency of the primary alcohol and methyl ester (**41** and **42**). Additional tethers were also examined but were found to be less optimal (**18** and **43**−**44**). The 2,5-disubstituted furan was found to be a suitable phenyl isostere (**45**).

With our optimized P_1 substituent in hand, we were now able to reexamine the SAR of the P_3 substituent.

Table 3. Selectivity of Representative Nitriles

cmpd	cat B IC_{50} (nM)	cat L IC_{50} (nM)	cat S IC_{50} (nM)
20	34 000[a]	170[b]	226[a]
21	496 ± 108	31 ± 1.6	48 ± 4.5
3	45 ± 7.6	6 ± 3.6	88[b]
39	1.8 ± 0.75	20 ± 7.6	46 ± 5.0
10	6.8 ± 0.6	554[b]	937[b]

[a] $n = 1$. [b] $n = 2$.

We discovered that with the 3-carboxy-O-benzylserine P_1 substituent in place, dramatic potency enhancement was observed regardless of the P_3 subsituent. In fact, substituents that afforded little potency in compounds with only hydrogen at P_1 were now nanomolar inhibitors (compare **27** with **48**, **28** with **49**, and **30** with **10**). As before, the benzyl ether tether was found to be optimal (**10** and **14**), and the carboxylate functionality was shown to improve potency (**50**). With the more potent 2-fluoro-4-chlorobenzoyl group at P_3, we again saw potency improvement upon incorporation of the O-benzylserine P_1 substituent and then upon meta-carboxylation (**28**, **46**, and **47**).

Because our structure-based approach was directed specifically at cat B, we were optimistic that we could achieve selectivity over other cysteine proteases. Table 3 lists potency data obtained for representative nitriles against cathepsins B, L, and S. Compound **20**, a very weak cat B inhibitor, was found to be relatively potent against cat L and S. Incorporation of the diphenylacetyl group at P_3 (**21**) improved activity against all three enzymes, although the effect was more pronounced for cat B than the others. Subsequent optimization of the P_2 position (**3**) provided a compound that was modestly selective for cat B over cat S but not cat L. Incorporation of the tethered benzoate substituent at P_1 yielded a compound with selectivity for cat B over both cat L and cat S (**39**). However, the most dramatic effect was observed upon replacement of the diphenylacetyl substituent of compound **39** with a smaller group, such as in compound **10**. As discussed previously, this modification has a modest effect on cat B potency. However, we see a substantial loss of activity against both cat L and cat S. This results in ~100-fold selectivity for cat B over the other enzymes.

These compounds were confirmed to be reversible inhibitors of cat B. This was demonstrated by forming a complex by preincubating the enzyme in the presence of excess inhibitor (compounds **10** and **39**) and measuring enzyme activity after dialysis and dilution into the assay mixture containing substrate. In both cases, enzyme activity was fully restored.

Conclusion

The work described herein represents a successful application of the principles of structure-based drug design to the optimization of a series of peptidyl nitrile inhibitors of cat B. Through systematic, iterative optimization of the substituents at the P_3, P_2, and P_1 positions, we were able to achieve a ~1000-fold improvement in potency from our original lead compound. High-quality X-ray crystallography of the complex of one of our first nanomolar inhibitors (**3**) bound to the enzyme confirmed the hypothesized mode of nitrile inhibition and enabled further optimization of the

template. The value of the molecular modeling tools employed in this study was demonstrated by the excellent agreement of modeling results with X-ray data. Of particular note was the achievement of high potency and selectivity through optimization of S′ site binding interactions. A carboxylate group tethered from the P_1 position was oriented to make a salt-bridge interaction with the histidine-containing loop of the S_2' site. Even in the absence of an X-ray structure of compound **39** or one of its analogues bound to cat B, the SAR data provides a high degree of confidence that our predicted structural model was reflective of the actual inhibitor binding mode. Additional support for this conclusion can be found in the high selectivity observed for the inhibition of cat B over other cathepsins. In conclusion, we utilized structural information to guide us in the optimization of a high-micromolar lead compound (**19**) into selective, low nanomolar cat B inhibitors. For example, compound **10**, while exhibiting low nanomolar inhibition of cat B, was only weakly potent against cathepsins L and S. Because of the absence of structural data on cathepsins S and L, it is not possible to discuss the structural basis of isozyme selectivity.

Experimental Section

Determination of Inhibition of Cathepsin B Activity. Recombinant human cat B protein was expressed in baculovirus and purified as described elsewhere.[31] To a microtiter well was added 100 uL of a 20 μM solution of inhibitor in assay buffer (0.1 M, pH 5.8, phosphate buffer containing ethylenediaminetetraacetic acid (1.33 mM), dithiothreitol (2.7 mM), and Brij (0.03%)) followed by 50 μL of a 6.4 mM solution of Z-Arg-Arg-AMC substrate (Peptides International) in assay buffer. After the solution was mixed, 50 uL of a 0.544 nM solution of recombinant human cat B in assay buffer was added to the well, yielding a final inhibitor concentration of 10 μM. Enzyme activity was determined by measuring fluorescence of the liberated aminomethylcoumarin at 460 nM using 355 nM excitation, at 20 min. Percent enzyme inhibition was determined by comparison of this activity to that of a solution containing no inhibitor. Compounds that showed >50% inhibition at 10 μM were subsequently subjected to a dose response curve analysis, and IC_{50}'s were determined.

Chemistry. Melting points (mp) were determined on a Thomas−Hoover melting point apparatus and are uncorrected. ^{1}H NMR spectra were recorded on a Bruker DPX-300 spectrometer. Mass spectroscopy (MS) analyses were perfomed on a Micromass Platform electrospray mass spectrometer, using positive ionization. Microanalyses were performed at Robertson Laboratory, Inc., Madison, NJ. All organic solvents used were of anhydrous grade. All reactions were run under a positive pressure of nitrogen unless otherwise stated. Chromatographic separations were performed with silica gel 60. Compounds were dried by suspension of anhydrous $MgSO_4$, followed by vacuum filtration.

***N*-(*tert*-Butoxycarbonyl)-3-methylphenylalanine (2).** To 1.1 g of sodium hydride (1.82, 60% dispersion in mineral oil, washed with hexane, 46 mmol) suspended in anhydrous dimethylformamide (DMF, 125 mL), at room temperature under a N_2 atmosphere, was added diethyl *tert*-butoxycarbonylaminomalonate (**1**, 11.1 g, 40 mmol, 10.2 mL) dropwise. After 2 h at ambient temperature, *m*-methylbenzylbromide (7.5 g, 40 mmol, 5.5 mL) was added dropwise, and the reaction was stirred at ambient temperature for 2 h. The reaction mixture was adjusted to pH 5 with acetic acid (0.4 mL), and 2.0 mL of water was added. It was stirred in a 150 °C bath under gentle reflux for 16 h. After the solution cooled to room temperature, $NaHCO_3$ (4.55 g, 54 mmol) dissolved in water (250 mL) was added followed by 2.5 mL of Alcalase 2.4 L (Novo Nordisk BioChem, ID no. 119878). After 2.5 h at 25−27 °C, 150 mL of ethyl ether was added and stirring continued for 1 h. The reaction mixture was extracted twice with ethyl ether. The aqueous layer was cooled to 0 °C and acidified to pH 3 with 6 N HCl. The mixture was extracted with ethyl acetate (3 × 100 mL), which was washed with water and brine, dried ($MgSO_4$), and evaporated and chromatographed (silica gel, 5% MeOH, CH_2Cl_2) to yield **2** (3.55 g, 63% yield). $[\alpha]_D$ + 17.46° ($CHCl_3$). ^{1}H NMR (300 MHz, $CDCl_3$): δ 12.60 (1H, s); 6.90−7.20 (5H, m); 4.03−4.12 (m, 1H); 2.96 (1H, dd, J = 13.5, 4.5 Hz); 2.77 (1H, dd, J = 13.5, 10.5 Hz); 2.26 (3H, s); 1.32 (9H, s).

***N*-Cyanomethyl-*N*α-(diphenylacetyl)-3-methylphenylalaninamide (3).** To a solution of **2**, (5.0 g, 17.92 mmol), HOBT (3.29 g, 21.5 mmol), and *N*-methylmorpholine (7.9 mL, 7.25 g, 71.7 mmol) in CH_2Cl_2 (100 mL) was added EDCI (5.15 g, 26.9 mmol) in one portion, and the solution was stirred at room temperature for 16 h. The solution was then diluted with CH_2Cl_2 (150 mL), washed with HCl (2 × 250 mL), saturated aqueous $NaHCO_3$ (250 mL), and brine (100 mL), dried ($MgSO_4$), and evaporated to yield 5.37 g of a white solid, which was taken up in formic acid (64 mL) and stirred at room temperature for 6 h. The formic acid was then evaporated under high vacuum at room temperature. The residue was dissolved in water (25 mL), basified with saturated aqueous $NaHCO_3$, and extracted with ethyl acetate (3 × 80 mL). The combined organic layers were then washed with brine (50 mL) and evaporated to yield *N*-cyanomethyl-*N*α-(*tert*-butoxycarbonyl)-3-methylphenylalaninamide as a brown oil. (1.86 g, 48% for 2 steps). ^{1}H NMR (300 MHz, $CDCl_3$): δ 7.90 (1H, br s); 7.22 (1H, t, 7.5 Hz); 6.96−7.14 (4H, m); 4.20 (2H, d, J = 6.0 Hz); 3.67 (1H, dd, J = 9.0, 4.1 Hz); 3.22 (1H, dd, J = 14.0, 4.1 Hz); 2.71 (1H, dd, J = 14.0, 9.0); 2.33 (3H, s). To a solution of this material (0.21 g, 0.92 mmol) and *N*-methylmorpholine (0.30 mL, 2.8 g, 2.76 mmol) in CH_2Cl_2 (10 mL) was added diphenylacetyl chloride (0.20 g, 0.92 mmol) in one portion. After it was stirred for 2 h, the solution was diluted with CH_2Cl_2 (40 mL) and then washed with 1 N HCl (50 mL) and brine (50 mL) and then evaporated and chromatographed (silica, 50−75% ethyl acetate/hexane) to yield **3** as a white solid, mp 169−170 °C (0.32 g, 85% yield). ^{1}H NMR (300 MHz, $CDCl_3$): δ 7.22−7.38 (8 H, m); 6.98−7.18 (6H, m); 6.85 (1H, br s); 6.80 (1H, d, J = 7.1 Hz); 6.19 (1H, d, J = 6.5 Hz); 4.87 (1H, s); 4.83 (2H, d, J = 6.1 Hz); 3.79 (1H, dd, J = 17.3, 6.0 Hz); 3.63 (1H, dd, J = 17.3, 6.0 Hz); 3.02 (1H, dd, J = 14.03, 6.5 Hz); 2.89 (1H, dd, J = 14.0, 8.0 Hz); 2.27 (3H, s). MS (*m*/*z*): (M + H) 412. Anal. Calcd for $C_{26}H_{25}N_3O_2$: C, H, N.

Compounds **19**−**32** and **34**−**37** were prepared in a manner similar or identical to that for compound **3**.

***N*-Cyanomethyl-*N*α-methyl-*N*α-(diphenylacetyl)-3-methylphenylalaninamide (5).** To a solution of NaH (60% in mineral oil, 39 mg, 0.98 mmol) in DMF (2 mL) was added a solution of **4** (0.30 g, 0.98 mmol) in DMF (3 mL) dropwise, over 5 min. The mixture was then stirred at room temperature for 10 min, after which time iodomethane (0.14 g, 61 uL, 0.98 mmol) was added in one portion. After it was stirred for 16 h, the solution was quenched with water (5 mL) and poured into saturated aqueous LiCl (50 mL). The mixture was extracted with ethyl acetate (3 × 20 mL), and the combined organic phases were washed with saturated aqueous LiCl (2 × 50 mL), dried over $MgSO_4$, and evaporated. The residue was chromatographed (silica, 10% ethyl acetate/hexane) to yield *N*-(*tert*-butoxycarbonyl)-*N*-methyl-3-methylphenylanine ethyl ester as a white solid (0.19 g, 60% yield). ^{1}H NMR (300 MHz, $CDCl_3$, mixture of rotamers): δ 7.12−7.21 (1H, m); 6.91−7.06 (3H, m); 4.93 (0.5H, dd, J = 11.4, 4.5 Hz); 4.56 (0.5H, dd, J = 12.2, 4.5 Hz); 3.72 (1.5H, s); 3.71 (1.5H, s); 3.19−3.31 (1H, m); 2.90−3.04 (1H, m); 2.71 (1.5H, s); 2.70 (1.5H, s); 2.32 (3H, s); 1.39 (4.5H, s); 1.32 (4.5H, s). This material was dissolved in ethyl acetate (15 mL) and cooled to 0 °C. HCl was then bubbled into the solution for 1 min. The solution was warmed to room temperature, stirred for 0.5 h, and then evaporated to dryness.

The residue was taken up in CH_2Cl_2 (15 mL), and *N*-methylmorpholine (0.19 mL, 0.178 g, 0.18 mmol) was added, followed by diphenylacetyl chloride (0.14 g, 0.59 mmol), and the solution was stirred at room temperature for 2 h, after which time it was washed with 1 N HCl (50 mL) and brine (50 mL), dried ($MgSO_4$), and evaporated to yield 0.21 g of material. This residue was next dissolved in a 2:1 tetrahydrofuran (THF)/methanol mixture (3 mL), followed by addition of 1 N aqueous NaOH (0.56 mL, 0.56 mmol). After the solution was stirred for 1 h at room temperature, the THF and methanol were evaporated, and the residue was acidified with 1 N HCl. The aqueous phase was then extracted with ethyl acetate (3 × 30 mL). The organic phases were washed with water (50 mL) and brine (50 mL), dried ($MgSO_4$), and evaporated to yield 0.20 g of crude product, which was taken up in CH_2Cl_2 (10 mL), followed by the addition of *N*-methylmorpholine (0.29 mL, 0.26 g, 2.62 mmol) and HOBt (88 mg, 0.58 mmol) and EDCI (0.15 g, 0.79 mmol). After it was stirred for 16 h at room temperature, the solution was washed with 1 N HCl (50 mL), saturated aqueous $NaHCO_3$ (50 mL), and brine (50 mL), dried ($MgSO_4$), evaporated, chromatographed (5% diethyl ether/CH_2Cl_2), and recrystallized (ethyl acetate/hexane) to yield **5** as a white solid, mp 153−154 °C (84 mg, 32% yield for 4 steps). ^{1}H NMR (250 MHz, $CDCl_3$): δ 6.80−7.35 (14H, m); 5.38 (1H, dd, J = 7.0, 5.7 Hz); 5.10 (1H, s); 3.94 (1H, dd, J = 17.8, 6.3 Hz); 3.63 (1H, dd, J = 17.8, 5.7 Hz); 3.16 (1H, dd, J = 12.0, 6.3 Hz); 2.97 (1H, dd, J = 12.6, 6.3 Hz); 2.90 (3H, s); 2.28 (3H, s). MS (*m*/*z*): (M + H) 426. Anal. Calcd for $C_{27}H_{27}N_3O_2$: C, H, N.

Allyl 3-(Iodomethyl)benzoate (7). A solution of 3-(chloromethyl)benzoic acid **6** (50.0 g, 0.293 mol), potassium carbonate (48.61 g, 0.352 mol), and allyl bromide (50.7 mL, 0.586 mol) in acetone (500 mL) was refluxed for 2 h, after which time the solution was cooled to room temperature and filtered through Celite. The filtrate was evaporated, and the residue was chromatographed (silica, 5% ethyl acetate/hexane) to yield 54.74 g of a mixture of allyl 3-(chloromethyl)benzoate and allyl 3-(bromomethyl)benzoate as a clear oil. This was taken up in acetone (500 mL), and sodium iodide (46.56 g, 0.311 mol) was added in one portion. The mixture was stirred for 6.5 h, after which time the mixture was filtered. The filtrate was evaporated, and the residue was dissolved in diethyl ether (500 mL), washed with water (1 × 200 mL), 5% sodium sulfite solution (1 × 200 mL), and brine (1 × 200 mL), dried over magnesium sulfate, and evaporated to yield **7** as a white solid, which was used directly (66.66 g, 76% yield for 2 steps). ^{1}H NMR (300 MHz, $CDCl_3$): δ 8.06 (1H, t, J = 1.8 Hz); 7.94 (1H, dt, J = 7.9, 1.5 Hz); 7.58 (1H, dt, J = 7.9, 1.5 Hz); 7.38 (1H, d, J = 7.6 Hz); 5.95−6.12 (1H, m); 5.42 (1H, dq, J = 17.1, 1.5 Hz); 5.31 (1H, dq, J = 10.4, 1.5 Hz); 4.83 (2H, dt, J = 6.8, 1.2 Hz); 4.48 (3H, s).

***O*-[[3-(Allyloxycarbonyl)phenyl]methyl]-*N*-(*tert*-butoxycarbonyl)-L-serinamide (8).** Sodium hydride (7.5 g, 60% in mineral oil, 187 mmol) was washed with dry pentane (2 × 20 mL) to remove the mineral oil and then suspended in anhydrous DMF (150 mL). To this suspension at 0 °C was added *N*-butoxycarbonyl-L-serine (19.2 g, 93.7 mmol) dropwise with vigorous stirring. The mixture was stirred for an additional 5 min at 0 °C and then at room temperature for 30 min. The solution was cooled back down to 0 °C, and a solution of **7** (28.3 g, 93.7 mmol) in DMF (150 mL) was added dropwise over 15 min. The mixture was then warmed to room temperature for 30 min. DMF was evaporated under high vacuum (bath temperature < 40 °C), and the residue was diluted with water (500 mL) and washed with ether (2 × 400 mL). The aqueous layer was then acidified with 1 N HCl to pH 3 and extracted with ethyl acetate (3 × 100 mL). The organic layers were washed with brine (200 mL) and then dried ($MgSO_4$) and evaporated to yield crude *O*-[[3-(allyloxycarbonyl)phenyl]-methyl]-*N*-(*tert*-butoxycarbonyl)-L-serine as a yellowish oil (11.43 g). A solution of this material (22.6 g, 59.6 mmol) and *N*-methylmorpholine (19.7 mL, 179 mmol) in CH_2Cl_2 (400 mL) was cooled to −10 °C, and isobutyl chloroformate (8.52 mL, 65.6 mmol) was added dropwise over 10 min. After the solution was stirred for 15 min, ammonia gas was bubbled into the solution at a moderately vigorous rate for 15 min at −10 °C. The solution was then warmed to room temperature and stirred for 30 min. The reaction mixure was cooled to 0 °C, and 1 N HCl (500 mL) was added. The organic phase was washed with 1 N HCl (2 × 300 mL), washed with saturated $NaHCO_3$ (500 mL), dried ($MgSO_4$), and then evaporated in vacuo to yield **8** as a clear oil (14.53 g, 21% for 2 steps). ^{1}H NMR (300 MHz, $CDCl_3$): δ 7.95−8.03 (2H, m); 7.39−7.55 (2H, m); 6.42 (1H, br s); 5.95−6.12 (1H, m); 5.62 (1H, br s); 5.40 (1H, dq, J = 17.1, 1.5 Hz); 5.29 (1H, dq, J = 10.4, 1.5 Hz); 4.82 (1H, dt, J = 5.8, 1.5 Hz); 4.64 (1H, d, J = 11.9 Hz); 4.56 (1H, d, J = 11.9 Hz); 3.93 (1H, dd, J = 9.2, 3.7 Hz); 3.60 (1H, dd, J = 9.2 Hz, 6.4 Hz), 1.44 (9H, s).

(*s*)-2-Amino-3-(3-allyloxycarbonylphenyl)methoxypropionitrile (9). To dry DMF (50 mL) at 0 °C was added oxalyl chloride (9.55 g, 6.56 mL, 75.24 mmol) slowly, via syringe. The mixture was then stirred at 0 °C for 5 min, after which time pyridine (12.2 mL, 150.48 mmol) was added in one portion, followed by **8** (14.22 g, 37.62 mmol) in DMF (50 mL). The mixture was stirred at 0 °C for 45 min, then diluted with ethyl acetate (600 mL), washed with saturated aqueous LiCl (3 × 600 mL), and dried over $MgSO_4$. Evaporation of solvent, followed by chromatography (silica, 35% ethyl acetate/hexane), yielded crude (*s*)-2-(*tert*-butoxycarbonylamino)-3-(3-allyloxycarbonylphenyl)methoxypropionitrile as a clear oil (11.78 g, 87% yield). ^{1}H NMR (300 MHz, $CDCl_3$): δ 8.00−8.05 (2H, m); 7.60 (1H, d, J = 8.9 Hz); 7.47 (1H, t, J = 7.5 Hz); 5.97−6.12 (1H, m); 5.42 (dq, 1H, J = 17.4, 1.5 Hz); 5.30 (1H, dq, J = 10.5, 1.5); 4.84 (2H, dt, J = 5.7, 1.5 Hz); 4.77 (1H, br s); 4.67 (2H, s); 3.74 (1H, dd, J = 9.5, 3.7 Hz); 3.67 (dd, 1H, J = 9.5, 4.2 Hz); 1.45 (9H, s). This material was dissolved in formic acid (125 mL), and the solution was stirred at room temperature for 6 h, after which time the formic acid was evaporated at 25 °C. The residue was then dissolved in water (50 mL), basified with saturated aqueous $NaHCO_3$, and extracted with ethyl acetate (3 × 150 mL). The combined organic layers were then washed with water (50 mL) and brine (50 mL), dried ($MgSO_4$), and evaporated to yield **9** as a light yellow oil, which was utilized without further purification (7.73 g, 91% yield). ^{1}H NMR (300 MHz, $CDCl_3$): δ 8.00−8.05 (2H, m); 7.57−7.62 (1H, m); 7.46 (1H, t, J = 6.9 Hz); 5.98−6.12 (1H, m); 5.42 (1H, dq, J = 17.4, 1.5 Hz); 5.30 (J = 10.5, 1.5 Hz); 4.83 (2H, d, J = 5.7); 4.67 (2H, s); 3.89 (1H, br s); 3.68 (2H, dd, J = 3.0, 1.5 Hz); 1.45 (9H, s).

***N*-[2-[(3-Carboxyphenyl)methoxy]-1(*S*)-cyanoethyl]-3-methyl-*N*α-(2,4-difluorobenzoyl)-L-phenylalaninamide (10).** To a solution of **2** (3.22 g, 11.54 mmol) and **9** (3.0 g, 11.54 mmol) in CH_2Cl_2 (100 mL) was added *N*-methylmorpholine (3.8 mL, 34.6 mmol), followed by HOAt (1.88 g, 13.8 mmol) and EDCI (3.32 g,17.3 mmol), and the solution was stirred overnight at room temperature The solution was then washed with 1 N HCl (100 mL), saturated $NaHCO_3$ (100 mL), and brine (100 mL), dried ($MgSO_4$), evaporated, and chromatographed (silica, 25% ethyl acetate/hexane) to yield *N*-[2-[(3-(allyloxycarbonyl)phenyl)methoxy]-1(*S*)-cyanoethyl]-3-methyl-*N*α-(*tert*-butoxycarbonyl)-L-phenylalaninamide as a white solid (4.36 g, 72% yield). ^{1}H NMR (300 MHz, $CDCl_3$): δ 8.02 (1H, d, J = 7.4 Hz); 7.96 (1H, s); 7.43−7.55 (2H, m); 7.26−7.22 (1H, m); 7.02 (3H, m); 6.56 (1H, d, J = 8.6 Hz); 5.98−6.12 (1H, m); 5.42 (1H, dd, J = 17.3, 1.2 Hz); 5.30 (1H, dd, J = 17.3, 1.0 Hz); 5.20 (1H, br s); 4.99−5.04 (1H, m); 4.84 (1H, dd, J = 5.7 Hz); 4.59 (2H, s); 4.31 (1H, q, J = 4.31); 3.68 (1H, dd, J = 9.8, 3.7 Hz); 3.56 (1H, dd, J = 9.8, 4.2 Hz); 3.01 (2H, d, J = 6.01 Hz); 2.30 (3H, s); 1.39 (9H, s). This compound was taken up in formic acid (50 mL) and stirred at room temperature for 6 h, after which time the formic acid was evaporated at 25 °C. The residue was then dissolved in water (50 mL), basified with saturated aqueous $NaHCO_3$, and extracted with ethyl acetate (3 × 50 mL). The combined organic layers were then washed with water (50 mL) and brine (50 mL), dried ($MgSO_4$), and evaporated to yield *N*-[2-[(3-(allyloxycarbonyl)phenyl)methoxy]-1(*S*)-cyanoethyl]-3-methyl-L-phenylalaninamide as a clear oil, which was utilized without further purification (3.5 g, 100%

yield). ^{1}H NMR (300 MHz, $CDCl_3$): 8.11−8.17 (1H, m); 8.00−8.06 (2H, m); 7.42−7.59 (2H, m); 7.20 (1H, t, J = 8.0 Hz); 7.97−7.09 (3H, m); 5.97−6.11 (1H, m); 5.42 (1H, dd, J = 17.3, 1.2 Hz); 5.30 (1H, dd, J = 17.3, 1.0 Hz); 5.05−5.12 (1H, m); 4.83 (2H, dt, J = 5.7, 1.5 Hz); 4.68 (1H, d, J = 12.1); 4.62 (1H, d, J = 12.1); 3.75 (1H, dd, J = 9.4, 3.7 Hz); 3.66 (1H, dd, J = 9.4, 3.8 Hz); 3.58 (1H, dd, J = 9.8, 4.5 Hz); 3.20 (1H, dd, J = 12.7, 4.2 Hz); 2.62 (1H, dd, J = 12.7, 8.5 Hz); 2.31 (3H, s). To a solution of this product (0.25 g, 0.59 mmol) in CH_2Cl_2 (20 mL) was added *N*-methylmorpholine (0.18 g, 0.20 mL, 1.78 mmol), followed by 2,4-difluorobenzoyl chloride (0.10 g, 0.073 mL, 0.59 mmol). After the solution was stirred for 2 h at room temperature, the solution was washed with 1 N HCl (25 mL), saturated $NaHCO_3$ (25 mL), and brine (20 mL), dried over $MgSO_4$, evaporated, and chromatographed (silica, 1% methanol/CH_2Cl_2) to yield *N*-[2-[(3-(allyloxycarbonyl)phenyl)methoxy]-1(*S*)-cyanoethyl]-*N*α-(2,4-difluorobenzoyl)-L-3-methylphenylalaninamide as a white solid (0.263 g, 79% yield). ^{1}H NMR (300 MHz, $CDCl_3$): 7.95−8.05 (2H, m); 7.90 (1H, s); 7.15−7.50 (4H, m); 6.76−7.10 (6H, m); 5.97−6.11 (1H, m); 5.42 (1H, dd, J = 17.3, 1.2 Hz); 5.30 (1H, dd, J = 17.3, 1.0 Hz); 4.97−5.05 (1H, m); 4.80−4.89 (3H, m); 4.54 (2H, m); 3.62 (1H, dd, J = 9.8, 3.3 Hz); 3.56 (1H, dd, J = 9.8, 4.1 Hz); 3.20 (1H, dd, J = 13.6, 6.4 Hz); 3.08 (1H, dd, J = 13.6, 7.6 Hz); 2.30 (3H, s). A solution of this product (0.43 g, 0.76 mmol) and morpholine (0.66 g, 0.66 mL, 7.62 mmol) in THF (25 mL) was deoxygenated with bubbling N_2 for 10 min, followed by addition of $Pd(PPh_3)_4$ (0.088 g, 0.076 mmol), and the solution was stirred at room temperature for 30 min. THF was evaporated, and the residue was dissolved in ethyl acetate (50 mL), washed with 1 N HCl (50 mL) and brine (30 mL), dried ($MgSO_4$), evaporated, and chromatographed (silica, 2−4% MeOH/CH_2Cl_2) to yield **10** as an off-white solid, mp 126−128 °C (0.245 g, 60% yield). ^{1}H NMR (300 MHZ, $CDCl_3$): 8.02 (1H, s); 7.94 (1H, d, J = 7.6 Hz); 7.67−7.75 (1H, m); 7.59−7.64 (1H, m); 7.45 (1H, t, J = 7.9 Hz); 6.99−7.15 (6H, m); 5.05 (1H, t, J = 5.3 Hz); 4.78 (1H, t, J = 6.5 Hz); 4.67 (2H, s); 3.74 (2H, d, J = 5.3 Hz); 3.14 (1H, dd, J = 13.5, 6.4 Hz); 3.01 (1H, dd, J = 7.9 Hz); 2.29 (3H, s). MS (*m*/*z*): (M + NH_4^+) 539. Anal. Calcd for $C_{28}H_{24}F_2N_3O_5$: C, H, N.

Compounds **38**−**42**, **45**−**49**, and **50** were all prepared in a manner similar or identical to that described for compound **10**.

(*S*)-2-(*tert*-Butoxycarbonylamino)-5-(3-carbomethoxyphenyl)-4-pentynoic Acid (12). *N*-Boc-propargylglycine methyl ester[1] **11** (74.2 g, 0.33 mol), methyl 3-bromobenzoate (70.21 g, 0.33 mol), and CuI (2.47 g, 0.013 mmol) were dissolved in triethylamine (1 L), which was deoxygenated with bubbling N_2 for 2−3 min. *Bis*-(triphenylphosphine)palladium(II) dichloride (4.59 g, 0.0065 mol) was added, and the solution was refluxed for 2 h. The residue was then evaporated, diluted with ethyl acetate (740 mL), washed with 1 N HCl (2 × 300 mL), brine (200 mL), and saturated $NaHCO_3$ (300 mL), dried ($MgSO_4$), evaporated, and chromatographed (10% ethyl acetate/hexane) to yield (*R*,*S*)-2-(*tert*-butoxycarbonylamino)-5-(3-carbomethoxyphenyl)-4-pentynoic acid methyl ester as a clear oil (66.7 g, 56% yield). ^{1}H NMR (300 MHz, $CDCl_3$): 8.03−8.06 (1H, m); 7.92−7.98 (1H, m); 7.52−7.58 (1H, m); 7.36 (1H, t, J = 7.9 Hz); 5.39 (1H, br d, J = 8.0 Hz); 4.52−4.62 (1H, m); 3.91 (3H, s): 3.80 (1H, s); 2.92−2.98 (2H, m); 1.45 (9H, s). To this material in a mixture of acetonitrile (633 mL) and 0.2 M aqueous $NaHCO_3$ (1233 mL) was added Alcalase 2.4 L (Novo Nordisk, 8.0 mL), and the solution was stirred vigorously at room temperature for 2.5 h. The reaction mixture was then evaporated at 30 °C to remove acetonitrile, and the aqueous residue was washed with ether (3 × 350 mL). The aqueous phase was filtered through Celite, the pH was adjusted to 3 with 6 N HCl (∼57 mL), and the solution was extracted with ethyl acetate (9 × 100 mL). The combined organic layers were then dried ($MgSO_4$) and evaporated to yield **12** as a clear oil (25.2 g, 39.4%). ^{1}H NMR (300 MHz, $CDCl_3$): δ 8.02−8.05 (1H, m); 7.90−7.96 (1H, m); 7.51−7.57 (1H, m); 7.33 (1H, t, J = 7.9 Hz); 5.42−5.46 (1H, m); 4.56−4.65 (1H, m); 3.90 (3H, s); 2.97−3.03 (2H, m); 1.46 (9H, s). Mosher ester formation of free amine revealed >97% ee.

(*S*)-2-Amino-5-(3-carbomethoxyphenyl)pentanamide (13). To a solution of **12** (24.2 g, 69.6 mmol) in EtOH (540 mL) and THF (540 mL) was added 10% Pd/C (10.8 g), and the solution was hydrogenated under atmospheric pressure for 2 h. Filtration through Celite followed by evaporation yielded (*S*)-2-amino-5-(3-carbomethoxyphenyl)pentanoic acid as a clear oil (24.38 g, 99%). ^{1}H NMR: δ 7.81−7.90 (2H, m); 7.30−7.38 (2H, m); 5.03 (br d, J = 8.3 Hz); 4.32−4.40 (1H, m); 3.90 (3H, s); 2.63−2.72 (2H, m); 1.62−1.90 (4H, m); 1.45 (9H, s). To a solution of this material and *N*-methylmorpholine (21.1 g, 22.9 mL, 0.21 mol) in CH_2Cl_2 (300 mL) at −10 °C was added isobutyl chloroformate (9.45 g, 9.02 mL, 6.94 mol) dropwise over 10 min, and the solution was stirred at −10 °C for 10 min. Ammonia gas was then bubbled through the solution at a moderately vigorous rate for 15 min, and the solution was warmed to room temperature over 2 h. The solution was then washed with 1 N HCl (3 × 1 L) and saturated $NaHCO_3$ (300 mL). The organic phase was evaporated, and the residue was crystallized from ether/hexane to yield (*S*)-2-(*tert*-butoxycarbonylamino)-5-(3-carbomethoxyphenyl)pentanamide as a white solid (17.6 g, 73%). ^{1}H NMR (300 MHz, $CDCl_3$): δ 7.81−7.90 (2H, m); 7.30−7.38 (2H, m); 6.07 (1H, br s); 5.48 (1H, br s); 5.00 (1H, br d, J = 8.6 Hz); 4.06−4.13 (1H, m); 3.89 (3H, s); 2.60−2.72 (2H, m); 1.62−1.90 (4H, m); 1.42 (9H, s). To a portion of this material (3.0 g, 8.6 mmol) in ethyl acetate (100 mL) at 0 °C was bubbled HCl gas for 15 min, after which time solvent was evaporated, yielding **13** as a white solid (2.44 g), which was taken on directly to the subsequent step. ^{1}H NMR (MeOH): δ 7.82−7.95 (2H, m); 7.33−7.50 (2H, m); 3.90 (3H, s); 3.82−2.92 (1H, m); 2.76 (2H, t, J = 6.5 Hz); 1.73−1.98 (4H, m).

***N*-(5-(3-Carboxyphenyl)-1(*S*)-cyanopentyl]-3-methyl-*N*α-(2,4-difluorobenzoyl)-L-phenylalaninamide (14).** Compounds **2** (2.51 g, 8.76 mmol) and **13** (2.44 g, 8.76 mmol) were coupled as described for the preparation of **10** to yield a white solid (4.44 g), which was, without purification, diluted in DMF (25 mL) and added to the solution created by the addition of oxalyl chloride (2.2 g, 1.52 mL, 17.4 mmol) to DMF (20 mL) at 0 °C, followed by the addition of pyridine (2.75 g, 2.81 mL, 34.8 mmol). The resulting brown solution was stirred at 0 °C for 1.5 h, then diluted with ethyl acetate (200 mL), and washed with saturated aqueous LiCl (3 × 300 mL), dried ($MgSO_4$), evaporated, and chromatgraphed (25−35% ethyl acetate/hexane), followed by recrystallization (ether/hexane) to yield *N*-(5-(3-carbomethoxyphenyl)-1(*S*)-cyanopentyl]-3-methyl-*N*α-(*tert*-butoxycarbonyl)-L-phenylalaninamide as a white solid (2.5 g, 59% for 3 steps). ^{1}H NMR (300 MHz, $CDCl_3$): 7.87−7.92 (1H, m); 7.82 (1H, br s); 7.32−7.41 (2H, s); 7.15−7.21 (1H, m); 6.96−7.06 (2H, m); 6.17 (1H, br d, J = 7.5 Hz); 4.77−4.85 (1H, m); 3.92 (3H, s); 2.95−3.10 (2H, m); 2.65−2.70 (2H, m); 2.31 (3H, s); 1.66−1.76 (2H, m); 1.40 (9H, s). This material was deprotected and acylated as described for compound **10** to yield *N*-(5-(3-carbomethoxyphenyl)-1(*R*,*S*)-cyanopentyl]-3-methyl-*N*α-(2,4-difluorobenzoyl)-L-phenylalaninamide as a clear oil. ^{1}H NMR: 8.78 (1H, td, J = 9.0, 6.8 Hz); 7.85 (1H, dt, J = 7.2, 1.5 Hz); 7.77 (1H, br s); 7.15−7.35 (4H, m); 6.82−7.08 (4H, m); 6.53 (1H, d, J = 8.3 Hz); 4.73−4.85 (1H, m); 3.90 (3H, s); 3.19 (1H, dd, J = 14.0, 6.8 Hz); 3.09 (1H, dd, J = 14.0, 8.0 Hz); 2.60−2.67 (2H, m); 2.28 (3H, s); 1.62−1.76 (4H, m). To a solution of this compound (0.46 g, 0.83 mmol) in THF (40 mL) was added potassium trimethylsilanoate (316 mg, 2.5 mmol), and the solution was stirred at room temperature overnight, during which time substantial yellow precipitate formed. The solvent was evaporated, and the residue was dissolved in ethyl acetate (75 mL) and washed with 1 N HCl (75 mL), dried ($MgSO_4$), evaporated, and chromatographed (2% MeOH/CH_2Cl_2, 0−0.05% HOAc) to yield **14** as a white solid, mp 170−172 °C (0.30 g, 70% yield). ^{1}H NMR (CD_3OD): δ 7.82−7.87 (2H, m); 7.65−7.74 (1H, m); 7.32−7.46 (2H, m); 6.98−7.18 (6H, m); 4.80 (1H, t, J = 7.0 Hz); 4.71 (1H, t, J = 7.0 Hz); 3.12 (1H, dd, J = 13.4, 7.1 Hz); 3.01 (1H, dd, J = 13.4, 7.1 Hz); 2.66−2.74

(2H, m); 2.29 (3H, s); 1.70−1.89 (4H, m). MS (*m*/*z*): (M + H) 520. Anal. Calcd for $C_{29}H_{27}F_2N_3O_4$: C, H, N.

Compound **43** was prepared in a manner similar to compound **14**.

Methyl 3-(2-Iodoethoxy)benzoate (16). To methyl 3-hydroxybenzoate **15** (5.0 g, 32.9 mmol) in acetone (100 mL) was added 1,2-dibromoethane (11.3 mL, 131.4 mmol) and K_2CO_3 (5.45 g, 39.4 mmol), and the solution was refluxed 16 h. TLC showed an incomplete reaction, so acetone was evaporated and DMF (100 mL) was added. The solution was then heated to 60 °C for 16 h. After the solution was cooled and filtered, the solution was evaporated, and the residue was chromatographed (25% ethyl acetate/hexane) to yield methyl 3-(2-bromoethoxy)benzoate as a clear oil, which was then diluted in acetone (50 mL). NaI (2.78 g, 18.52 mmol) was added, and the solution was refluxed for 2 h. The cooled solution was filtered, dissolved in ethyl acetate (50 mL), washed with 5% aqueous Na_2SO_3 (50 mL), water (50 mL), and brine (50 mL), dried ($MgSO_4$), and evaporated to yield **16** as a clear oil (2.7 g, 27% for 2 steps). ^{1}H NMR (250 MHz, $CDCl_3$): δ 7.63−7.68 (1H, m); 7.53−7.57 (1H, m); 4.68 (2H, t, J = 6.8 Hz); 4.92 (3H, s); 3.44 (2H, t, J = 6.8 Hz).

4-(3-Carbomethoxyphenoxy)-2-aminobutyronitrile (17). A 1 M solution of $Na(TMS)_2$ in THF (8.82 mL, 8.82 mmol) was added to a solution of *N*-(diphenylmethylene)aminoacetonitrile (1.9 g, 8.65 mmol) in THF (90 mL) at −78 °C via syringe and stirred for 30 min. A solution of **16** (2.7 g, 8.82 mmol) in THF (30 mL) was added dropwise, and the solution was warmed to room temperature over 3 h. The solution was quenched with saturated NH_4Cl (50 mL) and extracted with ethyl acetate (3 × 50 mL). The organic layers were washed with water (50 mL) and brine (50 mL), dried ($MgSO_4$), evaporated, and chromatographed (12.5% ethyl acetate/hexane). The purified product was then diluted in Et_2O (90 mL), and 1 N HCl (7.5 mL, 7.5 mmol) was added, followed by vigorous stirring for 16 h. The ether layer was separated, and the aqeous layer was washed with Et_2O (3 × 50 mL), basified to pH 8 with saturated $NaHCO_3$, and extracted with ethyl acetate (3 × 50 mL). The organic layer was washed with brine (50 mL), dried ($MgSO_4$), and evaporated to yield **17** as a clear oil (1.48 g, 73% for 2 steps). ^{1}H NMR (250 MHz, $CDCl_3$): 7.60−7.68 (1H, m); 7.52−7.57 (1H, m); 7.53 (1H, t, J = 6.8 Hz); 7.05−7.13 (1H, m); 4.02−4.33 (3H, m); 3.92 (3H, s); 2.05−2.35 (2H, m).

***N*-[2-[(3-Carboxyphenoxy]-1(*S*)-cyanopropyl]-3-methyl-*N*α-(diphenylacetyl)-L-phenylalaninamide (18).** Compound **17** was converted to *N*-[2-[(3-carbomethoxyphenoxy]-1(*S*)-cyanopropyl]-3-methyl-*N*α-(diphenylacetyl)-L-phenylalaninamide, using a procedure similar to that described for **14**. To a solution of this material (0.16 g, 0.27 mmol) in THF (3 mL) was added a solution of $LiOH·H_2O$ (22 mg, 0.54 mmol) in water (0.5 mL). The mixture was stirred for 6 h, after which time additional water (1 mL) was added, and the solution was stirred for an additional 1 h. The mixture was concentrated, diluted in water (20 mL), acidified with 1 N HCl, and extracted with ethyl acetate (3 × 30 mL). The combined organic layers were washed with brine, dried ($MgSO_4$), evaporated, and chromatographed (5% MeOH/CH_2Cl_2, 0.05% AcOH) to yield **18** as a white solid (35 mg), mp 169−170 °C. NMR indicated that the product was, as expected, a 1:1 mixture of diastereoisomers. ^{1}H NMR (DMSO, 250 MHz): δ 7.50−7.56 (1H, m); 7.31−7.42 (2H, m); 6.82−7.28 (15 H); 5.03 (0.5H, s); 5.01 (0.5H, s); 4.82−4.91 (1H, m); 4.44−4.56 (1H, m); 2.68−295 (2H, m); 2.08−2.28 (2H, m); 2.19 (1.5H, s); 2.13 (1.5H, s); 3.91−4.14 (2H, m). MS (*m*/*z*): (M + H) 574. Anal. Calcd for $C_{33}H_{33}N_3O_5·0.5\ H_2O$: C, H, N.

Crystallization and Data Collection. A complex was formed by incubation of a 4-fold molar excess of compound **3** with 1.5 mg of cat B in binding buffer (20 mM sodium acetate pH 5.5, 300 mM KCl and 75 mM NaCl) plus 2 mM 1,4-dithiothreitol for 30 min at room temperature. The complex was buffer exchanged four times into binding buffer with 25 μM compound **3** using an Amicon Centricon-10 concentrator and finally concentrated to 10 mg/mL. Crystals were grown by the hanging-drop vapor diffusion method by mixing equal volumes of protein solution and well buffer (50 mM Na acetate pH 5.5, 100 mM KCl, and 15−20% monomethyl ether PEG 5000 at 4 °C). Crystals were cryo-protected at room temperature by a 15 min, 10 step transfer to a cryobuffer solution (50 mM Na acetate pH 5.5, 100 mM KCl, 50 mM NaCl, 20% monomethyl ether PEG 5000, 14% ethylene glycol, 10% glycerol) with 20 μM compound **3** and immediately flash-frozen in a 100 K nitrogen gas cold stream (Low Temp System, MSC) for data collection. Diffraction data were collected on an R-AXIS-IIc image-plate system (Molecular Structures Corp.) with "Yale-style" double focusing mirrors on an RU-2HR generator (MSC) operating at 104 mA and 50 kV. A complete data set was collected from a single crystal maintained at 100 K. The images were indexed and integrated using Denzo/Scalepack.[32]

Structure Determination and Refinement. The structure was determined by molecular replacement using XPLOR[33] (MSI, Inc.) with a structure of human cat B as the search model. After independent rigid-body refinement of the 3 cat B proteins in the asymmetric unit, the electron density for the inhibitor was clearly seen in each of the active sites. Several rounds of iterative model building with the program O,[34] positional refinement, individual B refinement, and addition of waters were conducted before adding the three inhibitors to the model. The active site of one complex was fully solvent accessible, while the active site of the other two complexes were buried by crystal contacts. The electron density for the inhibitor of the exposed active site indicated that the occupancy may have been less than 1.0. The occupancy of each inhibitor was refined, and the occupancies of 1.0, 1.0, and 0.78 were used in the model. The final model contained 3 cat B/compound **3** complexes, and 535 waters with an *R* factor of 16.9% in the resolution range of 6.0−1.9 Å. Recently, the model was further refined in preparation for deposition and to exploit the power of R_{free}, monolayer refinement, and bulk solvent in CNX[35] (MSI, Inc.). The final CNX model was indistinguishable from the original XPLOR model in the active site; summary statistics for the CNX refined model are in the Supporting Information. The model has been submitted to the Protein Data Bank, accession no. 1GMY.[36]

Supporting Information Available: Crystallographic parameters for the structure of the cat B−**3** complex. This material is available free of charge via the Internet at http://pubs.acs.org.

References

(1) Turk, B.; Turk, D.; Turk, V. Lysosomal cysteine proteases: more than scavengers. *Biochim. Biophys. Acta* **2000**, *1477*, 98−111.
(2) Chapman, H. A.; Riese, R. J.; Shi, G. P. Emerging roles for cysteine proteases in human biology. *Annu. Rev. Physiol.* **1997**, *59*, 63−88.
(3) Barrett, A. J.; Kirschke, H. Cathepsin B, Cathepsin H, and Cathepsin L. *Methods Enzymol.* **1981**, *80C*, 535−561.
(4) Berquin, I. M.; Sloane, B. F. Cathepsin B expression in human tumors. *Adv. Exp. Med. Biol.* **1996**, *389*, 281−294.
(5) Petanceska, S.; Burke, S.; Watson, S. J.; Devi, L. Differential distribution of messenger RNAs for cathepsins B, L, and S in adult rat brain: an in situ hybridization study. *Neuroscience* **1994**, *59*, 729−738.
(6) Keyszer, G.; Redlich, A.; Haupl, T.; Zacher, J.; Sparmann, M.; Entgethum, U.; Gay, S.; Burmester, G. R. Differential expression of cathepsins B and L compared with matrix metalloproteinases and their respective inhibitors in rheumatoid arthritis and osteoarthritis: a parallel investigation by semiquantitative reverse transcriptase-polymerase chain reaction and immunohistochemistry. *Arthritis Rheum.* **1998**, *41*, 1378−1387.
(7) Buttle, D. J.; Handley, C. J.; Ilic, M. Z.; Saklatvala, J.; Murata, M.; Barrett, A. J. Inhibition of cartilage proteoglycan release by a specific inactivator of cathepsin B and an inhibitor of matrix metalloproteinases. Evidence for two converging pathways of chondrocyte-mediated proteoglycan degradation. *Arthritis Rheum.* **1993**, *36*, 1709−1717.
(8) Esser, R. E.; Angelo, R. A.; Murphey, M. D.; Watts, L. M.; Thornburg, L. P.; Palmer, J. T.; Talhouk, J. W.; Smith, R. E. Cysteine proteinase inhibitors decrease articular cartilage and bone destruction in chronic inflammatory arthritis. *Arthritis Rheum.* **1994**, *37*, 236−247.
(9) Veber, D. F.; Thompson, S. K. The therapeutic potential of advances in cysteine protease inhibitor design. *Curr. Opin. Drug Discovery Dev.* **2000**, *3*, 362−369.

(10) Otto, H. H.; Schirmeister, T. Cysteine Proteases and Their Inhibitors. *Chem. Rev.* **1997**, *97*, 133−171.
(11) Thompson, S. K.; Smith, W. W.; Zhao, B.; Halbert, S. M.; Tomaszek, T. A.; Tew, D. G.; Levy, M. A.; Janson, C. A.; D'Alessio, K. J.; McQueney, M. S.; Kurdyla, J.; Jones, C. S.; DesJarlais, R. L.; Abdel-Meguid, S. S.; Veber, D. F. Structure-Based Design of Cathepsin K Inhibitors Containing a Benzyloxy-Substituted Benzoyl Peptidomimetic. *J. Med. Chem.* **1998**, *41*, 3923−3927.
(12) Yamashita, D. S.; Smith, W. W.; Zhao, B.; Janson, C. A.; Tomaszek, T. A.; Bossard, M. J.; Levy, M. A.; Oh, H. J.; Carr, T. J.; Thompson, S. K.; Ijames, C. F.; Carr, S. A.; McQueney, M.; D'Alessio, K. J.; Amegadzie, B. Y.; Hanning, C. R.; Abdel-Meguid, S.; DesJarlais, R. L.; Gleason, J. G.; Veber, D. F. Structure and Design of Potent and Selective Cathepsin K Inhibitors. *J. Am. Chem. Soc.* **1997**, *119*, 11351−11352.
(13) Brisson, J. R.; Carey, P. R.; Storer, A. C. Benzoylamidoacetonitrile is bound as a thioimidate in the active site of papain. *J. Biol. Chem.* **1986**, *261*, 9087−9089.
(14) Dufour, E.; Storer, A. C.; Menard, R. Peptide aldehydes and nitriles as transition state analogue inhibitors of cysteine proteases. *Biochemistry* **1995**, *34*, 9136−9143.
(15) Drenth, J.; Kalk, K. H.; Swen, H. M. Binding of chloromethyl ketone substrate analogues to crystalline papain. *Biochemistry* **1976**, *15*, 3731−3738.
(16) Picken, P. P.; Guthrie, D. J.; Walker, B. Inhibition of bovine cathepsin B by amino acid-derived nitriles. *Biochem. Soc. Trans.* **1990**, *18*, 316.
(17) Several patent applications covering peptidyl nitrile inhibitors of various cathepsins have appeared recently, but none contain potency data. WO 0119816, WO 0049007, WO 0049008, WO 9924460.
(18) Falgueyret, J. P.; Oballa, R. M.; Okamoto, O.; Wesolowski, G.; Aubin, Y.; Rydzewski, R. M.; Prasit, P.; Riendeau, D.; Rodan, S. B.; Percival, M. D. Novel, Nonpeptidic Cyanamides as Potent and Reversible Inhibitors of Human Cathepsins K and L. *J. Med. Chem.* **2001**, *44*, 94−104. This very recent reference describes a series of cyanamides that are quite distinct chemically from aminonitriles.
(19) Berger, A.; Smolarsky, M.; Kurn, N.; Bosshard, H. R. A new method for the synthesis of optically active amino acids and their N derivatives via acylamino malonates. *J. Org. Chem.* **1973**, *38*, 457−460.
(20) Kijima, T.; Ohshima, K.; Kise, H. Facile optical resolution of amino acid esters via hydrolysis by an industrial enzyme in organic solvents. *J. Chem. Technol. Biotechnol.* **1994**, *59*, 61−65.
(21) Abood, N. A.; Nosal, R. Zinc mediated addition of active halides to a glycine cation equivalent. *Tetrahedron Lett.* **1994**, *35*, 3669−3672.
(22) Laganis, E. D.; Chenard, B. L. Metal silanolates. *Tetrahedron Lett.* **1984**, *25*, 5831−5834.
(23) O'Donnell, M. J.; Eckrich, T. M. The synthesis of amino acid derivatives by catalytic phase-transfer alkylations. *Tetrahedron Lett.* **1978**, *25*, 4625−4628.
(24) Jia, Z.; Hasnain, S.; Hirama, T.; Lee, X.; Mort, J. S.; To, R.; Huber, C. P. Crystal Structures of Recombinant Rat Cathepsin B and a Cathepsin B−Inhibitor Complex. *J. Biol. Chem.* **1995**, *270*, 5527−5533. At the time this work was commenced in 1994, no human cat B−inhibitor complexes were publicly available. We therefore utilized this structure, to which we had exclusive access through a collaboration with the NRC of Canada.
(25) McMartin, C.; Bohacek, R. S. QXP: powerful, rapid computer algorithms for structure-based drug design. *J. Comput.-Aided Mol. Des.* **1997**, *11*, 333−344.
(26) Hasnain, S.; Hirama, T.; Huber, C. P.; Mason, P.; Mort, J. S. Characterization of cathepsin B specificity by site-directed mutagenesis. Importance of Glu245 in the S2−P2 specificity for arginine and its role in transition state stabilization. *J. Biol. Chem.* **1993**, *268*, 235−240.
(27) Musil, D.; Zucic, D.; Turk, D.; Engh, R. A.; Mayr, I.; Huber, R.; Popovic, T.; Turk, V.; Towatari, T.; Katunuma, N. The refined 2.15 A X-ray crystal structure of human liver cathepsin B: the structural basis for its specificity. *EMBO J.* **1991**, *10*, 2321−2330.
(28) Turk, D.; Podobnik, M.; Popovic, T.; Katunuma, N.; Bode, W.; Huber, R.; Turk, V. Crystal structure of cathepsin B inhibited with CA030 at 2.0-A resolution: A basis for the design of specific epoxysuccinyl inhibitors. *Biochemistry* **1995**, *34*, 4791−4797.
(29) Aronson, N. N. J.; Barrett, A. J. The specificity of cathepsin B. Hydrolysis of glucagon at the C-terminus by a peptidyldipeptidase mechanism. *Biochem. J.* **1978**, *171*, 759−765.
(30) Shaw, E.; Wikstrom, P.; Ruscica, J. An exploration of the primary specificity site of cathepsin B. *Arch. Biochem. Biophys.* **1983**, *222*, 424.
(31) Steed, P. M.; Lasala, D.; Liebman, J.; Wigg, A.; Clark, K.; Knap, A. K. Characterization of recombinant human cathepsin B expressed at high levels in baculovirus. *Protein Sci.* **1998,** 2033−2037.
(32) Otwinowski, Z.; Minor, W. Processing of X-ray Diffraction Data Collected in Oscillation Mode. In *Methods in Enzymology*; Carter, C. W., Sweet, R. M., Eds.; Academic Press: New York, 1997; Vol. 276, pp 307−325.
(33) Brünger, A. T. XPLOR, Version 3.1; Yale University Press: New Haven, CT, 1993.
(34) Jones, T. A.; Zou, J.-Y.; Cowan, S. W.; Kjeldgaard, M. Improved Methods for the Building of Protein Models in Electron Density Maps and the Location of Errors in these Models. *Acta Crystallogr.* **1991**, *A47*, 110−119.
(35) Brünger, A. T.; Adams, P. D.; Clore, G. M.; DeLano, W. L.; Gros, P.; Grosse-Kunstleve, R. W.; Jiang, J.-S.; Kuszewski, J.; Nilges, M.; Pannu, N. S.; Read, R. J.; Rice, L. M.; Simonson, T.; Warren, G. L. Crystallography and NMR system (CNS). *Acta Crystallogr.* **1998**, *D54*, 905−921.
(36) Berman, H. M.; Westbrook, J.; Feng, Z.; Gilliand, G.; Bhat, T. N.; Weissig, H.; Shindyalov, I. N.; Bourne, P. E. The Protein Data Bank. *Nucleic Acids Res.* **2000**, *28*, 235−242.

JM010206Q